

G-CSF treatment of chemotherapy induced
neutropenia - Online supplement

Eliezer Shochat and Vered Rom-Kedar

Weizmann Institute of Science

May 31, 2008

The online supplement begins with introducing the model and its parameters S.1 and continues with several sections that may be read independently of each other. In S.2 we explain why the *AMC* is an indicator for the neutropenia grade. In S.3 we provide a geometrical intuition for these arguments. In S.4 we discuss the accuracy of the proposed clinical estimates of the *AMC*. Finally, in S.5 we add more details regarding the Monte-Carlo simulations. These include additional simulations with different *AMC* values.

S.1 The mathematical model of the *GN* dynamics under chemotherapy

We use the following mathematical formulation to describe the G-CSF Neutrophils (*GN*) dynamics in the blood (see also Table 1 where all parameters are defined and specified):

$$\begin{cases} \frac{dG}{dt} = inG(t) + \frac{B_G^{max}}{1 + N/k_N} - D_G^r \cdot G - \frac{D_G^n \cdot N}{k_N + N} \cdot G \\ \frac{dN}{dt} = BNF(t) \frac{k_G + k_{NEF} G}{k_G + G} - D_N \cdot N \end{cases} \quad (\text{S.1.1})$$

The units are $[G] = pg/ml, [N] = \#cells/ml, [t] = day$. The pharmacokinetics of the subcutaneous injected *G* is calculated as: $inG(t) = \lambda \frac{dose_G}{v_d} e^{-\lambda t}$ where $dose_G$ is the daily *G* dose. For *CG*, $inG(t) = \frac{dose_G}{v_d}$.

The bone-marrow basic flux function $BNF(t)$, which is *G* independent, has been constructed phenomenologically to comply with the clinical observations. We assume in the model that normally $BNF(t) = B_N$ is a constant (listed in table 1). Furthermore, to comply with clinical observations regarding the response of the bone-marrow to chemotherapy, we assume it is depleted by a certain rate (represented by β_1), remains low (at *Bnadir*) for a period of time ($T_{stop} - T_{start}$) and then recovers with a certain rate (represented by β_2). Accordingly, we take the following form for the

flux function $BNF(t) = Bnadir + (B_N - Bnadir) \left(1 - \frac{\tanh(\beta_1(t-T_{start})) - \tanh(\beta_2(t-T_{stop}))}{2}\right)$, where $\tanh(x) = \frac{\exp(x) - \exp(-x)}{\exp(x) + \exp(-x)}$. Note that for sufficiently large $\beta_{1,2}(T_{stop} - T_{start})$, $Bnadir$ [*cells/ml/day*] is approximately the minimal value of $BNF(t)$. Finally, we note that the $BNF(t)$ five-parameter fit of the clinical data indicates that it is treatment specific (see Figs. 1,2 of the main manuscript).

S.2 The Acute Marrow Capacity (AMC) significance

Here we show that for the model (S.1.1) the depth of the neutrophils nadir and the G beneficial effect are both controlled by a single number, the dimensionless parameter AMC :

$$AMC = k_{NEF} \cdot \frac{Bnadir}{N^* \cdot D_N} \quad (S.2.1)$$

which we call the *acute marrow capacity* ($N^* = 5 \cdot 10^6 \text{ cells/ml}$ is a fixed scaling factor, k_{NEF} measures enhancement by G-CSF of the neutrophils flux from the bone marrow to the blood, and D_N measures the neutrophils blood clearance rate, see Table 1).

Indeed, first note that for a sufficiently large constant value of G , the N rate of change becomes $\frac{dN}{dt} \approx Bnadir k_{NEF} - D_N \cdot N = D_N \cdot (AMC \cdot N^* - N)$ (use the definition of AMC and notice that the first term in the second equation of (S.1.1) becomes essentially independent of G). Therefore, N converges to $N = AMC \cdot N^*$ (at the rate D_N). Hence, if $AMC > \frac{N_{tr}}{N^*} = 0.1$ the neutropenia can be managed by a dedicated control of G . More precisely, if G is held fixed then N converges to:

$$N_{fixedG} = N^* \cdot AMC \cdot \frac{k_G/k_{NEF} + G}{k_G + G}. \quad (S.2.2)$$

Now, if we require that N will converge to a value larger than the critical N ($N_{fixedG} > 0.1 \cdot N^* = N_{tr}$), then, we must hold G beyond a certain critical level ($G_{crit} = \frac{0.1 k_G k_{NEF} - 10 \cdot AMC}{AMC - 0.1}$). This requirement can be fulfilled only if $\frac{AMC}{3} > 0.1$. On the other hand, by the same

reasoning, if $AMC \leq 0.1$, G-CSF alone cannot reverse the neutropenia at the nadir. This reasoning has a lucid geometrical representation that is described next.

S.3 A phase-plane approach to GN dynamics.

The GN dynamics under various medical conditions with a fixed $BNF(t) = Bnadir$ may be summarized by one plot - the phase portrait of the (GN) system. This representation allows to capture several different clinical behaviors in a clear and concise manner and allows to better explain the reasoning behind the proposed change in protocol.

Plotting a *phase portrait* is a useful tool in the study of systems of ordinary differential equations. In this representation, the G-CSF and neutrophils levels at a given instant of time are used as coordinates for a point $(G(t), N(t))$ that evolves in the GN plane (Fig. Supp. 1). The simultaneous time dependent changes in G and N are thus represented by non-intersecting curves (trajectories) with arrow heads indicated every 8 hours and pointing in the direction of change. An equilibrium point is a state at which no change occurs. The unique stable equilibrium point of this system appears in Fig. Supp. 1 as the intersection of two null-clines (curves in the GN plane along which the instantaneous rate of change of one of the variables vanishes): the solid blue curve is the G null-cline ($\frac{dG}{dt} = 0$) and the solid red curve is the N null-cline ($\frac{dN}{dt} = 0$). The clinical meaning of the equilibrium being stable is that after a perturbation, such as a G-CSF injection, the neutrophils level N always returns to its equilibrium value. In the phase portrait this means that no matter where one starts in the GN plane, the trajectory always converges to the point of intersection of the two null-clines.

The significance of the sustained G-CSF treatment scheme may be explained by analyzing how the shape of the N null-cline for $BNF(t) = Bnadir$ depends on the parameters. First, notice that $N_{nc}(G) = N^* \cdot AMC \cdot \frac{k_G/k_{NEF} + G}{k_G + G}$ is an increasing function of G , attaining the value $N^* \frac{AMC}{k_{NEF}}$ at $G = 0$ and approaches the value $N_{asym} = AMC \cdot N^*$ as G becomes large. A smaller value of AMC corresponds to a shift and compression of

this curve downward (the dashed red, green and blue curves in Fig. Supp. 1, notice the logarithmic scale). This lowers the corresponding equilibrium point where these curves intersect the G null-cline (the solid blue curve). Thus, if AMC is too low (dashed green and blue curves), namely the bone marrow function is depressed, this intersection point lies below the threshold value of $N_{tr} = 0.1 \cdot N^*$ and without intervention the system always converges to a neutropenic state (blue trajectory). In such a situation, a pulsed G administration increases N only temporarily (purple and magenta trajectories).

Fixing a G value corresponds in this figure to a motion on a vertical line: starting with a low N value, N increases towards the intersection of this vertical line with the N null-cline. Since the N null-cline asymptotes the horizontal line N_{asym} we see that if this horizontal line is above the threshold value of $0.1 \cdot N^*$ then we can find a sufficiently large G beyond which N will cross the neutropenic level (cyan trajectory). If $N_{asym} < 0.1 \cdot N^*$ (below the dashed blue curve) no G support can reverse the neutropenia. Now, when $BNF(t)$ is recovering from its minimal value $Bnadir$ to its normal value, the G support may be stopped and the neutrophils will naturally rise to their pre-treatment values (continuation of the cyan trajectory).

Observe that the above geometrical arguments are robust - they do not depend on the exact form of the null-clines and the exact values of all parameters - all that matters is the monotone properties of the null-clines and their asymptotic form. This observation reflects the mathematical statement that the system (S.1.1) is structurally stable and thus small inaccuracies in the form of the rate functions do not change the basic properties of the solutions. Clinically, this means that small changes in the parameters that correspond to variability between different patients do not alter the essential features that are described above. The extensive Monte Carlo simulations demonstrate that even with the transient changes in $BNF(t)$ this robustness prevails.

S.4 The accuracy of the grade calculation from neutrophils counts.

We have shown that at the nadir $AMC \approx \frac{k_G + G}{k_G/k_{NEF} + G} \frac{N}{N^*}$. Since the measurement of N is readily available whereas G values are not regularly measured and k_G, k_{NEF} are a-priori unknown, a statistical approach regarding the possible distribution of G and a study of the variability in k_G, k_{NEF} is appropriate. Consider a log-Normal probability distribution of G : $P_g(G) = \frac{1}{\sigma G \sqrt{2\pi}} \exp(-(\ln G - \ln \bar{G})^2 / 2\sigma^2)$ with a mean at $\bar{G} = 1500 \text{ pg/ml}$ and a standard deviation $\sigma = 0.5$ (Fig. Supp. 2). Then, the probability distribution function of the AMC may be explicitly calculated as $P(AMC|N, k_{NEF}, k_G) = \frac{P_g(G(AMC; N, k_{NEF}, k_G))}{|\partial(AMC)/\partial G|}$ (since AMC is monotone in G and thus, for a fixed N and k_{NEF} , it has a single-valued inverse $G(AMC; N, k_{NEF}, k_G) = k_G \frac{AMC/k_{NEF} - N/N^*}{N/N^* - AMC}$). With some additional manipulations it can be shown that the mean value of AMC is of the form:

$$\langle AMC \rangle = \frac{N}{N^*} f(k_{NEF}, k_G, P_g(G))$$

where $f(k_{NEF}, k_G, P_g(G))$ is independent of N and its dependence on k_{NEF} is mild; for $\bar{G} = 1500 \text{ pg/ml}, \sigma = 0.5, k_G = 5000 \text{ pg/ml}$ and $k_{NEF} = (8, 10, 16)$ we obtain that $\langle AMC \rangle / (N/N^*) = (3.12, 3.35, 3.75)$ respectively. Allowing k_G to vary between $[3000 - 6000 \text{ pg/ml}]$ increases this interval to $(2.5 - 4.2)$. The approximate formula for AMC reflects this resulting expectation with $k_{NEF} = 10$ and $k_G = 5000 \text{ pg/ml}$. Further calculation shows that $|\partial(AMC)/\partial G|$ is small and leads, (despite possible large distributions in G), to narrow distributions in AMC (Fig. Supp. 2). In this figure we show the AMC distributions for three neutrophil counts: $N = 50 \cdot 10^3 \text{ cells/ml}$ - the borderline count between a \mathcal{G}_3 to a \mathcal{G}_2 grade, $N = 150 \cdot 10^3 \text{ cells/ml}$ - the \mathcal{G}_2 grade patients, and $N = 300 \cdot 10^3 \text{ cells/ml}$ - the borderline count between a \mathcal{G}_2 to a \mathcal{G}_1 grade. We see that even with the hypothetical wide distribution of G , the distributions at the borderline cases are definitive: the lower borderline case has only a minute fraction

with $AMC > 0.1$. On the other hand, for a k_G range of 4700 ± 700 pg/ml (an estimate reported in [1]), the upper borderline distribution has a relatively small fraction of patients with $AMC < 0.13$. Finally, for the intermediate regime, indeed a significant portion has AMC just above 0.1 and thus, may be helped by a sustained G-CSF treatment (whereas the standard G-CSF treatment will not suffice).

S.4.1 Monte-Carlo simulations of G-CSF treatment in \mathcal{G}_3 and \mathcal{G}_1 patients

To consolidate our confidence in the model performance we have repeated the Monte-Carlo simulation of the three treatment arms with 100 \mathcal{G}_3 patients ($AMC = 0.09$) and 100 \mathcal{G}_1 patients ($AMC = 0.14$). The results of these simulations are shown in Fig. Supp. 3 and Fig. Supp. 4.

In addition we estimate the risk of infection (IR) in each treatment arm for the two AMC levels (see Fig. Supp. 5 and Fig. Supp. 6). As expected, almost all \mathcal{G}_3 patients, regardless of the treatment arm, are at significant risk for infection: Placebo: $IR = 20\%$, SG : $IR = 19.9\%$ and the $pegG$ regimen cuts the risk only to $IR \approx 16\%$. These effects may explain the observed failure of G-CSF treatments in HDCT patients and stress the importance of additional support measures for these highly neutropenic patients.

On the other hand patients in the \mathcal{G}_1 group respond well to any G-CSF treatment. While the placebo control group remains at significant risk for infection: $IR = 20\%$, the risk for the SG group reduces dramatically to: $IR = 3\%$ and disappears all together for $pegG$ treated group ($IR = 0$). These effects may explain the observed success of the standard G-CSF treatments in lowering the duration of the neutropenia in conventional chemotherapy patients. We should also note that in practice we expect that the duration of the neutropenia for the \mathcal{G}_1 patients will be significantly shorter than the eight-ten days considered in our simulations. Such shorter period will further reduce the AUC_{500} of the placebo control group and will result in less significant difference between the IR

of the placebo and the *SG* arms.

We end the supplement with a few technical details regarding the Monte-Carlo simulations. In all the simulations we take the first 17 parameters that are listed in Table 2 to be log-normal distributed (see method section of the main text for the reasoning behind the parameter choices). The parameter B_{nadir} is then calculated as $B_{nadir} = \frac{AMC}{k_{NEF}} \cdot N^* \cdot D_N$, where AMC is fixed in each of the Monte-Carlo simulations. Notice that the resulting B_{nadir} is log-normal distributed as well, yet it is not independent of the other parameters.

References

- [1] Wang B, Ludden TM, Cheung EN, Schwab GG, Roskos LK. Population pharmacokinetic-pharmacodynamic modeling of filgrastim (r-metHuG-CSF) in healthy volunteers. *J Pharmacokinet Pharmacodyn* 2001;28:321–42.
- [2] Johnston E, Crawford J, Blackwell S, et al. Randomized, dose - escalation study of SD/01 compared with daily filgrastim in patients receiving chemotherapy. *J. Clin. Oncol* 2000;18:2522–8.
- [3] Shochat E, Rom-Kedar V, and Segel L, G-CSF control of neutrophil dynamics in the blood. *Bull Math Biol* 2007;69:2299–338.
- [4] Fenk R, Hieronimus N, Steidl U, et al. Sustained G-CSF plasma levels following administration of pegfilgrastim fasten neutrophil reconstitution after high-dose chemotherapy and autologous blood stem cell transplantation in patients with multiple myeloma. *Exp Hematol* 2006;34(10):1296–302.

Parameter	Meaning	Units	Values: G-CSF	Values: PegG
B_G^{max}	G max production rate	$pg/ml/day$	7000	7000
k_N	N dissociation constant	$cells/ml$	$0.5 \cdot 10^6$	$0.5 \cdot 10^6$
k_G	G MM constant	pg/ml	$5 \cdot 10^3$	$5 \cdot 10^3$
D_G^n	G elimination (by N)	1/day	6.93	4.08
D_G^r	G elimination (renal)	1/day	6	0.72
B_N	Basic normal flux of N	$\#cells/ml/day$	$15 \cdot 10^6$	$15 \cdot 10^6$
k_{NEF}	Enhancement of N flux by G	—	10	10
D_N	N clearance rate	1/day	3	3
λ	G absorption rate	1/day	4	0.5
v_d	volume of G distribution	ml	2300	4500

Table 1: Definition and values of model parameters used in the study. The parameters are fitted to the clinical control (without chemotherapy) data sets reported for SG [1] and $pegG$ [2] regimens. Note that B_N is the normal constant value of $BNF(t)$. The fitting method and the estimated parameters range is described in [3].

Parameter	Meaning	μ G-CSF	μ PegG	σ (G/PegG)
B_G^{max}	G max production rate	7000	7000	0.15
k_N	N dissociation constant	$0.5 \cdot 10^6$	$0.5 \cdot 10^6$	0.4
k_G	G MM constant	$5 \cdot 10^3$	$5 \cdot 10^3$	0.09
D_G^n	G elimination (by N)	6.93	4.08	0.34
D_G^r	G elimination (renal)	6	0.72	0.4
B_N	Basic normal flux of N	$15 \cdot 10^6$	$15 \cdot 10^6$	0.09
k_{NEF}	Enhancement of N flux by G	10	10	0.18
D_N	N clearance rate	3	3	0.18
λ	G absorption rate	4	0.5	0.09
v_d	volume of G distribution	2300	4500	0.18
$G(0)$	G initial value	50	50	0.09
$N(0)$	N initial value	$3 \cdot 10^6$	$3 \cdot 10^6$	0.09
w	Weight	70	70	0.09
T_{start}	Start of CT effect	2	2	0.01
T_{stop}	Stop of CT effect	17	17	0.01
β_1	Marrow depletion rate	0.25	0.25	0.01
β_2	Marrow recovery rate	0.25	0.25	0.01
B_{nadir}	(*) Marrow N flux at nadir= $\frac{AMC \cdot N^* D_N}{k_{NEF}}$	$\approx 160 \cdot 10^3$	$\approx 160 \cdot 10^3$	0.36

Table 2: Distribution of the model parameters used in the Monte-Carlo simulation. (*) Note that although the AMC is fixed, the marrow N flux at the nadir (B_{nadir}) varies due to variations in k_{NEF} and D_N ($N^* = 5 \cdot 10^6 cells/ml$ is fixed).

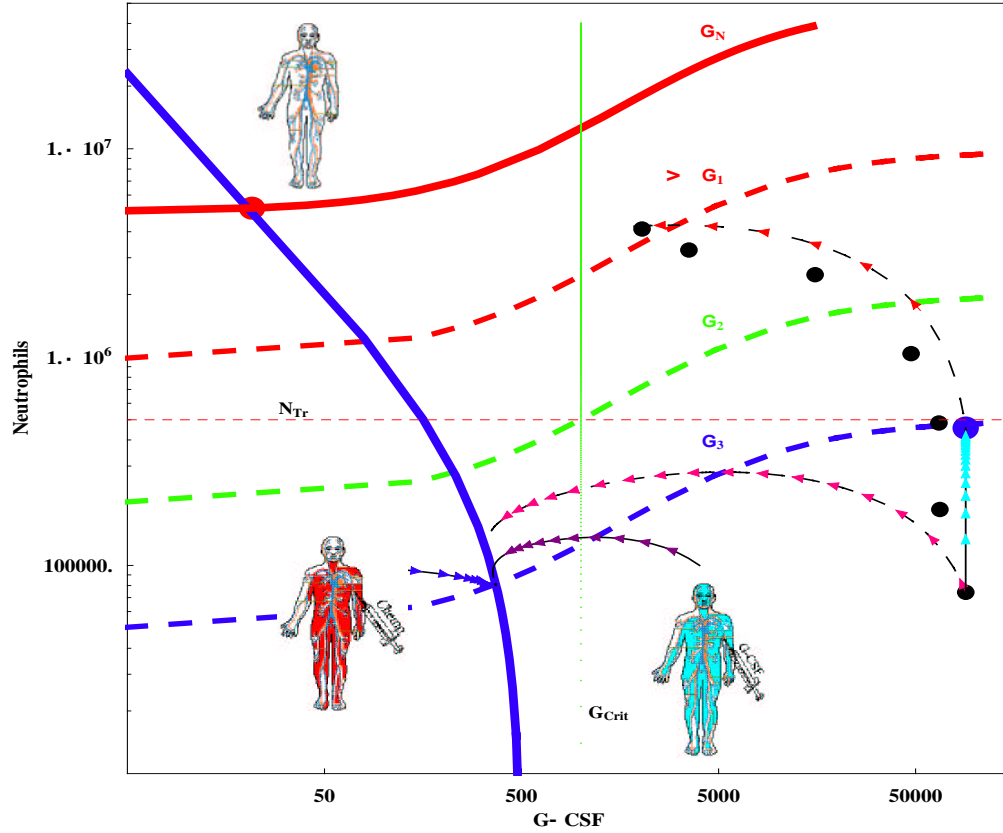


Figure Supp. 1: Chemotherapy induced GN dynamics phase portrait. The G null-cline (solid blue) and the N null-cline with normal AMC (\mathcal{G}_N) (solid red) intersect at $(G^*, N^*) \approx (50 \text{ pg/ml}, 5000 \cdot 10^3 \text{ cells/ml})$. The N null-clines for a mild neutropenic grade $> \mathcal{G}_1$, is represented by the dashed sigmoidal red line. The N null-clines for the typical \mathcal{G}_2 and \mathcal{G}_3 grades are represented by the dashed sigmoidal green and blue lines respectively. The critical level G_{Crit} of G -CSF for \mathcal{G}_2 grade patient is shown by a vertical green line which intersects with the \mathcal{G}_2 null-cline at the neutrophil threshold level ($N_{tr} = 500 \cdot 10^3 \text{ cells/ml}$). GN trajectories for a hypothetical \mathcal{G}_3 patient with no G -CSF treatment (natural dynamics) (blue), following a single pulse of standard (purple) and of high dose G -CSF (magenta, $15 \mu\text{g/kg/day}$) are shown. Alternatively, a cyan trajectory under a fixed G protocol throughout the marrow convalescence period is shown. It is followed (in dashed red) by a hypothetical natural recovery. Data points (black) of HDCT with $pegG$ treatment recovery phase (adapted from Fenk et al [4]), are provided for comparison.

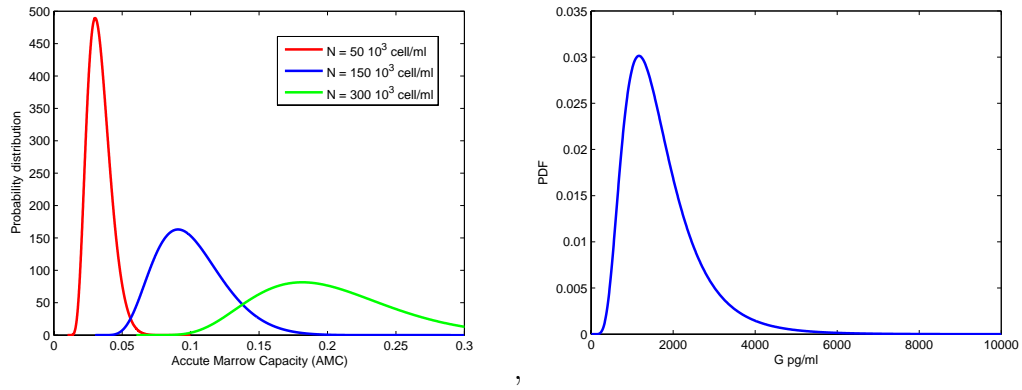


Figure Supp. 2: The probability distribution function of AMC (left). Here $k_{NEF} = 10$, and G is assumed to be Log-Normal distributed as shown on the right.

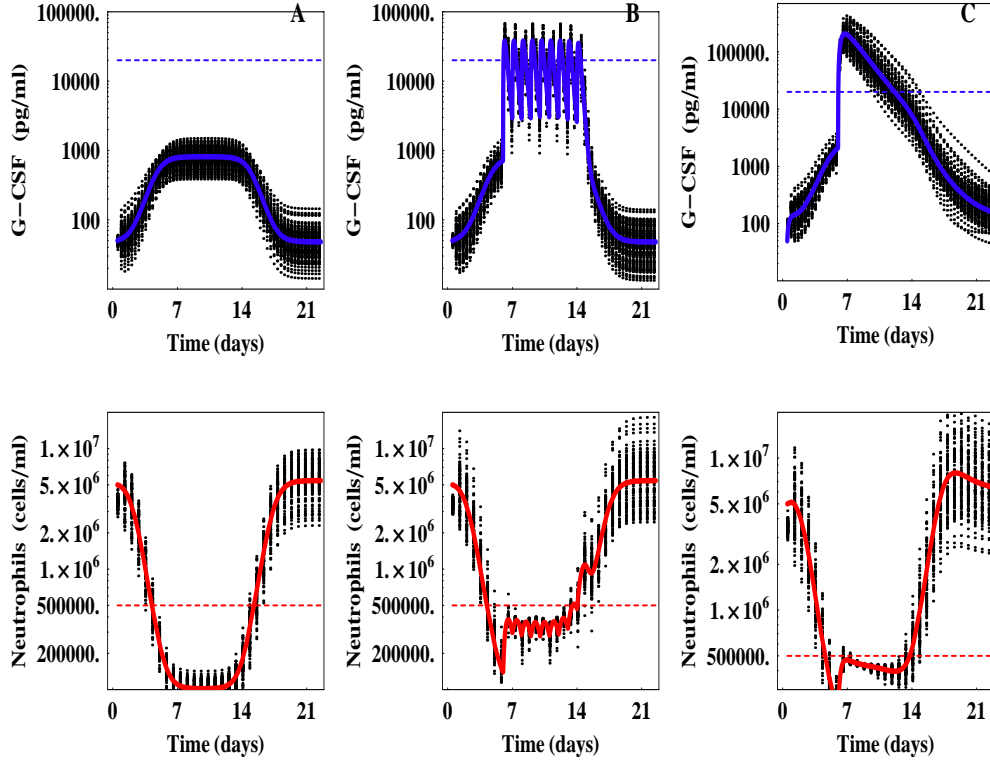


Figure Supp. 3: Clinical trial simulation of neutropenia treatment by placebo (**A**) and two G-CSF regimens: the standard Multi-pulsed (*sc*) *G* (**B**) and a single *pegG* (**C**) in \mathcal{G}_3 patients ($AMC = 0.09$). All other parameter values are as in Fig. 5 in the main text. We assume them to be independent, log-Normal distributed with $\sigma \approx 1.2$, mean values as in Table 1. $T_{stop} - T_{start} = 15days$, and $\beta_{1,2} = 0.08[1/day]$. Note the inability of any G-CSF protocol to salvage the neutropenia. We take the parameters distributions to be independent, although, theoretically, correlations between some of the parameters (e.g. between D_G^n and k_{NEF}) may be expected.

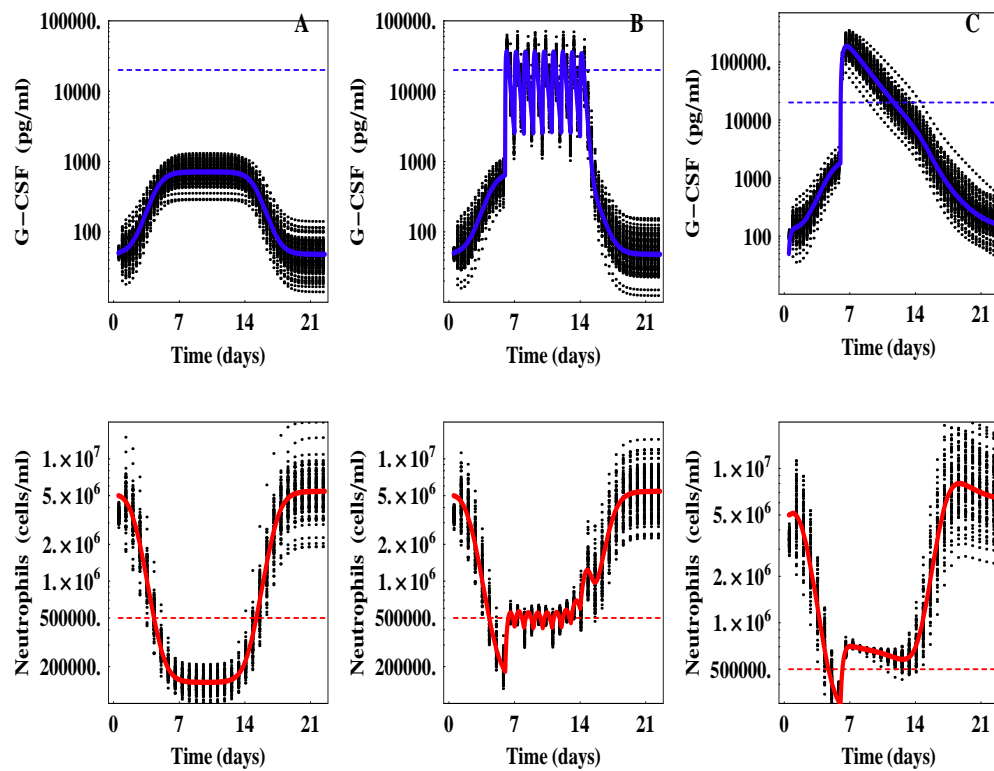


Figure Supp. 4: Clinical trial simulation of neutropenia treatment by placebo (**A**) and two G-CSF regimens: the standard Multi-pulsed (*sc*) *G* (**B**) and a single *pegG* (**C**) in \mathcal{G}_1 patients ($AMC = 0.14$). All other parameter values are as in Fig. 6 in the main text and in Fig. Supp. 3. Note the excellent therapeutic effect of the standard G-CSF protocol.

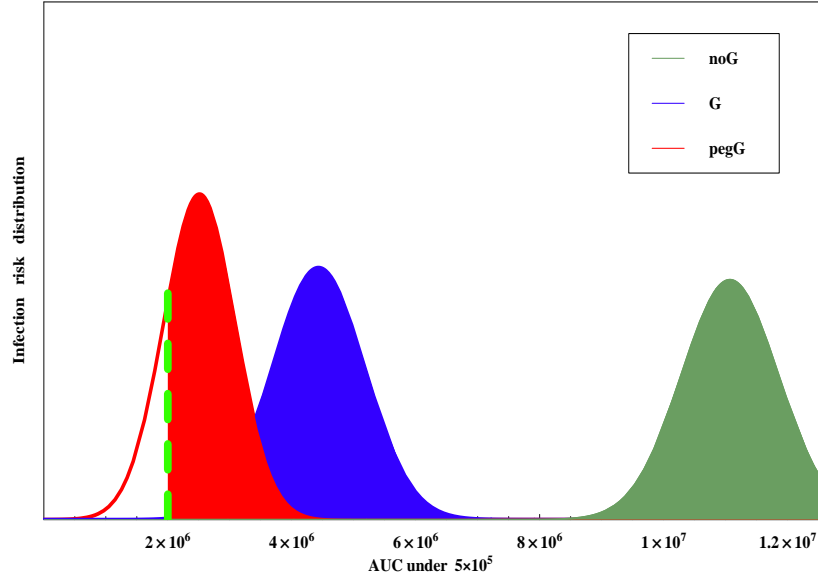


Figure Supp. 5: Probability distributions for the area under the curve, AUC_{500} , which is correlated with the risk of infection, for the three arms of Fig Supp. 3 in the \mathcal{G}_3 patients group. The shaded areas provide the probability that $AUC_{500} \geq 2 \cdot 10^6 [\text{days} \cdot \text{cells}/\text{ml}]$, taken as the probability to have a risk of infection $> 20\%$. Even though the distribution curves in each treatment arm are different from one another ($p < 0.001$ by the KS test) no treatment significantly reverts the risk of infection.

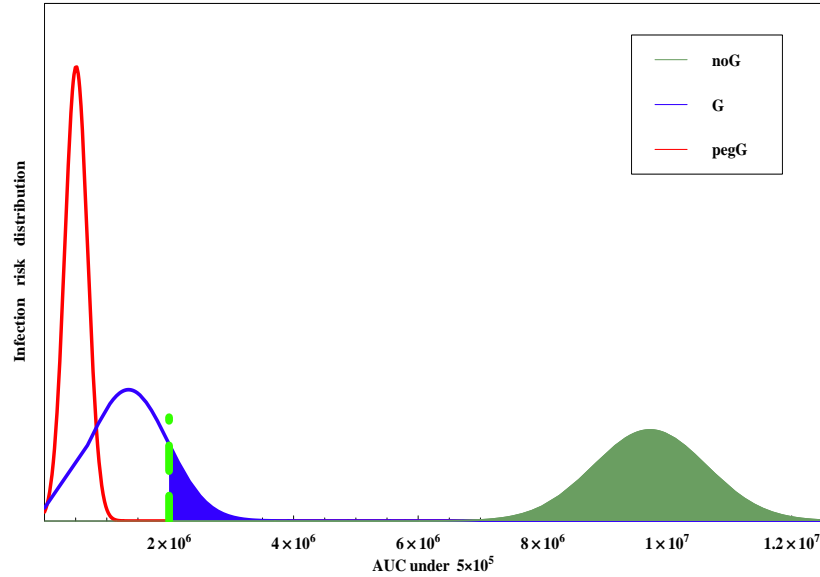


Figure Supp. 6: Probability distributions for the area under the curve, AUC_{500} , which is correlated with the risk of infection, for the three arms of Fig Supp. 4 in the \mathcal{G}_1 patients group. The shaded areas provide the probability that $AUC_{500} \geq 2 \cdot 10^6 [\text{days} \cdot \text{cells}/\text{ml}]$, taken as the probability to have a risk of infection $> 20\%$. The risk of infection in both *pegG* arm (red) and the standard G-CSF regimens are significantly lower than the placebo arm (green shade).